In-Situ DRIFT Spectroscopic Investigation on the Chemical Evolution of Zinc Phosphate Acid−Base Cement

Oliver Pawlig* and Reinhard Trettin

Institut für Geowissenschaften (Angewandte und Technische Mineralogie), Johannes Gutenberg−Universität, Saarstrasse 21, D-55099 Mainz, Germany

Received September 21, 1999. Revised Manuscript Received February 17, 2000

Diffuse reflectance infrared Fourier transform (DRIFT) spectroscopy has been used to follow the chemical evolution of zinc phosphate acid−base cement (ZPC), which has been prepared from unmodified, as well as from aluminum- and zinc-modified orthophosphoric acid. For the first time, amorphous dizinc cyclotetraphosphate octahydrate, $Zn_2P_4O_{12}\cdot 8H_2O$, although hydrolytically instable, has been observed as precursor phase prior to crystallization of α-hopeite, $\alpha\text{-}Zn_3(PO_4)_2\cdot 4H_2O$, in both systems. Within minutes from onset of mixing the infrared spectrum of unmodified ZPC is dominated by the characteristic vibrations of α-hopeite, due to matrix crystallization. Setting of modified ZPC is strongly affected by the presence of initially soluble aluminophosphate complexes, which form a hydrogel upon neutralization. Steric hindrance plays the key role in the sluggish crystallization kinetics of modified ZPC. The high compressive strength of modified ZPC is brought about by a condensed anion structure. Conceptionally, setting of ZPC consists of initial Lewis acid−base reactions and subsequent stages of hydration. In this work, it is shown that the tendency for the $Zn_2P_4O_{12}\cdot 8H_2O$ precursor phase to form is consistent with the Ostwald step rule of successive reactions.

Introduction

Acid−base cements are principally employed as luting agents in dentistry.[1−3] These materials provide the link between fixed prostheses, such as inlays, crowns, and bridges, and the supporting prepared tooth structure.[4−7] Traditionally, zinc phosphate cement (ZPC) has been the most popular among these materials. The success of prostheses fixed with ZPC has been well documented. A recent meta analysis of clinical data of 4118 conventional fixed partial dentures revealed an overall survival rate of 74.0 ± 2.1% after 15 years.[8] For ZPC, values for compressive strength of 80−150 MPa[9] and tensile strength of 5−8 MPa[10] have been reported, indicating that this material is adequate to resist masticatory stress. Moreover, hardened ZPC is extremely stiff and exhibits high modulus of elasticity of 13 GPa,[10] which permits the cement to resist elastic deformation in long span prostheses.[11] Material properties of ZPC are covered by international specifications.[12,13]

Typical cement powder of ZPC consists primarily of ZnO (80−90 wt %) and MgO (0−10 wt %). The current state of the art cement liquid, an aqueous solution of orthophosphoric acid (OPA), usually has a concentration of 45−60 wt %, and contains aluminum and zinc in a concentration range of 2−6 wt %.

Since dental cements are subjected to different kinds of constraints in oral environment, no luting agent is ideal for all situations. Principal factors of clinical magnitude are adequate mechanical and rheological properties, biocompatibility, low solubility, and an optimized setting time. Hence, to improve ZPC, additional modification, especially of the cement liquid, has been the subject of extensive research.[14−16]

Although ZPC is one of the most important materials used in modern dentistry its setting chemistry is not yet elucidated. However, to free modification from empiricism it is essential to have a sound understanding of chemical reactions taking place during setting. It is well-known that the early reaction products of freshly set ZPC are X-ray amorphous. A recent study about in-vivo matured cements has shown that α-hopeite recrystallizes from the amorphous matrix phase.[17] There is

(1) Wilson, A. D.; Nicholson, J. W. Acid−base Cements: Their Biomedical and Industrial Applications. In *Chemistry of Solid State Materials*; University Press: Cambridge, 1993; Vol. 3.
(2) Craig, R. G. *Restorative Dental Materials*; Mosby Inc.: St. Louis, 1993.
(3) Williams, D. Concise Encyclopedia of Medical and Dental Materials. In *Advances in Materials Science and Engineering*; Elsevier: Amsterdam, 1990; Vol. 5.
(4) Anstice, M. *Chem. Ind.* **1994**, *22*, 899.
(5) Jokstad, A.; Mjör, I. A. *J. Dent.* **1996**, *24*, 309.
(6) Nicholson, J. W. *Biomaterials* **1998**, *19*, 485.
(7) Diaz-Arnold, A. M.; Vargas, M. A.; Haselton, D. R. *J. Prosthet. Dent.* **1999**, *81*, 135.
(8) Creugers, N. H.; Kayser, A. F.; Van't Hoff, M. A. *Comm. Dent. Oral Epidemiol.* **1994**, *22*, 448.
(9) Branco, R.; Hegdahl, T. *Acta Odontol. Scand.* **1983**, *41*, 349.
(10) Bruce, W. L.; Stevens, L. *Austr. Dent. J.* **1989**, *34*, 132.
(11) Hussaini, S.; Wong, T. *J. Prosthet. Dent.* **1997**, *78*, 550.
(12) ISO 9917. *Dental Water-based Cements*, 1991.
(13) American National Standards Institute. *Specification No. 96 for Zinc Phosphate Cement;* American Dental Association: Chicago, 1991.
(14) Fardal, O.; Turnbull, R. S. *J. Am. Dent. Assoc.* **1986**, *112*, 863.
(15) Brackett, W. W.; Rosen, S. *Oper. Dent.* **1994**, *19*, 106.
(16) Li, J.; Forberg, S.; Söremark, R. *Acta Odontol. Scand.* **1994**, *52*, 209.
(17) Margerit, J.; Cluzel, B.; Leloup, J. M.; Nurit, J.; Pauvert, B.; Terol, A. *J. Mater. Sci. Mater. Med.* **1996**, *7*, 623.

10.1021/cm991148o CCC: $19.00
Published on Web 04/19/2000

still a lack of information about the formation and chemical nature of the intermediate amorphous phase as well as about its transformation to crystalline α-hopeite. For this reason we describe herein investigations on the chemical evolution of ZPC. Although ZPC is a complex system, the principal factor of setting and hardening is the reaction between zinc oxide and OPA. Therefore, this reaction was followed in situ by diffuse reflectance infrared Fourier transform (DRIFT) spectroscopy, using both, unmodified as well as modified OPA. Since OPA is an intrinsic part of the microstructure of ZPC cement paste, techniques that facilitate the study of wet specimens are necessary. In the past two decades DRIFT spectroscopy has been established as one of the most powerful spectroscopic techniques for the analysis of such samples since it is a rapid, matrix-free, and nondestructive method.[18−22]

Experimental Procedure and Analysis Technique

Materials. The powder of ZPC was made from plain ZnO (ACS grade, Fluka). For thermal deactivation the powder was roasted in air for 5 h at 1473 K and subsequently ground. The powder was sieved to yield particle sizes $d < 10\ \mu$m since high-quality DRIFT spectra can only be obtained when $d < \lambda$.[23] The specific surface area of the powder was measured to be 4.23 m^2/g using nitrogen gas adsorption (Micromeritics ASAP 2010). For use as unmodified cement liquid 50 wt % OPA was prepared by dilution from 85 wt % OPA (ACS grade, Fluka) which was used as received. The final concentration of the cement liquid was checked by specific gravity and electrical conductivity. A further 50 wt % OPA solution containing 3 wt % aluminum (grains, grade ≥ 99%, Fluka), and 3 wt % zinc was prepared by replacing the appropriate amount of water, so that for modified OPA an initial P/Al ratio of ∼4.6 was established. Deionized water used for dilution was high-resistance (conductivity less than 1 μS cm^{-1}) organics free.

Polycrystalline α-hopeite was synthesized by adding the stoichiometric amount of $Zn(CH_3COO)_2 \cdot 2H_2O$ to a 0.26 M OPA solution, adjusted to pH = 4.0 by addition of 2 M KOH solution. The precipitate was filtered and dried at 313 K during 24 h. $Zn_3(PO_4)_2 \cdot 2H_2O$ was obtained by heating α-hopeite to 423 K for 1 h in air. The residual water content was checked by thermogravimetry.

Instrumentation. DRIFT spectroscopic measurements were performed on a Paragon 1000 spectrometer using a diffuse reflectance accessory (both Perkin-Elmer). A KBr beam splitter for the mid-IR range and a mercury−cadmium−telluride (MCT) detector for sensitive and fast detection were used. For stabilization, the MCT detector was cooled with liquid nitrogen for about 2 h prior to data collection. Background and spectra were recorded with a nominal resolution of 4 cm^{-1}, averaging about 35 scans in the frequency range 4000−400 cm^{-1}. The Norton−Beer function was used for apodization. Second derivative spectra were calculated using a Savitzky−Golay filter algorithm.[24,25] Raman spectra were aquired using a Renishaw RM 1000 confocal Raman system, with a 514.5-nm argon ion laser as the excitation source and a Peltier cooled charge-coupled device detector. The incident laser power on the sample was limited to 3.1 mW to prevent sample damage. A ×20 Leica objective was used to focus the laser and to collect the backscattered light. Raman spectra were recorded without polarization in the continuous extended scan mode with an effective spectral resolution of 2.5 cm^{-1}, and a lateral resolution of about 15 μm in the range 1600−100 cm^{-1} by averaging 15 accumulations a 10 s. AFM measurements were performed in the noncontact mode under ambient atmosphere with a Topometrix Discoverer TMX 2010 atomic force microscope. Imaging was conducted by using silicon probes with a length of 226 μm, resonance frequencies in the 100−120 kHz range, and spring constants in the 36−71 N m^{-1} range. All measurements were performed in amplitude detection mode with feedback achieved at 50% of the free air resonance amplitude of the cantilevers. Scan speed was maintained at 400 nm s^{-1}. The Topometrix Discoverer software was used for the surface roughness analysis. Thermoanalysis was performed on a TG-DTA 92-16 thermobalance, and a DSC 131 (both Setaram), respectively. Samples of ZPC were heated in closed Pt (TG/DTA) and Al (DSC) crucibles at a heating rate of 10 K/min from 300 to 700 K under argon flow for thermogravimetric analysis, and nitrogen flow for DSC measurements.

Procedures. Cements were manually mixed on a clean cooled glass slab with a stainless steel dental spatula at 298 K and about 55% relative humidity using a powder-to-liquid ratio of 2.0. For each cement 1 g of powder was subdivided on the block into five equal parts. A part was mixed into 0.5 g of the OPA solution every 8 s. The total mixing time was 40 s. Spectral data were collected as soon as the cement could be placed as about 200 μm thin film on a 1 cm^2 stainless steel plate which was mounted on the sample base plate of the diffuse reflectance accessory. In DRIFT spectroscopy, the sampling depth of undiluted, highly opaque samples is in the range of 20−50 μm.[26] Hence, the condition of a sample of infinite depth is fulfilled here. After 8.5 min from the onset of mixing ZPC films were placed in an incubator at 310 K and 100% relative humidity. DRIFT spectroscopic measurements were repeated after 1 and 24 h. Afterward ZPC films were examined by nondestructive Raman spectroscopy and AFM. Subsequently the films were crushed and transferred to thermoanalysis. Vibrational spectra of α-hopeite and $Zn_3(PO_4)_2 \cdot 2H_2O$ were measured with a concentration of 5 wt % in a zinc oxide matrix using the powder sample cup of the DRIFT accesssory. DRIFT spectra of ZnO were measured using a KBr matrix (spectroscopic grade, Merck), employing an analyte concentration of 5 wt %.

Results and Discussion

DRIFT Spectra for the Reaction between Zinc Oxide and Unmodified OPA. The symmetry of a "free" PO_4^{3-} ion is T_d and the nine modes of internal vibrations span the representation $\Gamma_{vib}(T_d) = A_1 + E + 2F_2$. Here A_1 represents the symmetric stretching mode ν_s(P−O), located at ∼980 cm^{-1}, E represents the symmetric bending mode δ_s(OPO) at ∼420 cm^{-1}, and the triply degenerated F_2 modes represent the antisymmetric stretching mode ν_{as}(P−O) at ∼1100−1000 cm^{-1}, as well as the antisymmetric bending mode δ_{as}(OPO), located at ∼560 cm^{-1}, respectively.[27] All modes of vibration are Raman-active, but in IR only the F_2 modes are active. However, slight shifts of wavenumbers are expected to occur due to solid-state effects and the use of the DRIFT technique.[28,29] The broad and featureless bands in the DRIFT spectrum after 2.5 min (Figure 1a)

(18) Fuller, E. L.; Smyre, N. R. *Appl. Spectrosc.* **1990**, *44*, 451.
(19) Allen, T. J. *Vibr. Spectrosc.* **1992**, 3, 217.
(20) Ferraro, J. R.; Rein, A. J. Applications to Chemical Systems. In *Fourier Transform Spectroscopy*; Ferraro, J. R.; Basile, L. J., Eds.; Academic Press: Orlando **1985**; Vol. 4, p 253.
(21) Krishnan, K. In *Fourier Transform Infrared Spectroscopy, Industrial Chemical and Biochemical Applications*; Theophanides, T., Ed.; D. Reidel Publishing Company: Dordrecht, 1984; p 148.
(22) Korte, E. H.; Röseler, A. In *Infrared and Raman Spectroscopy, Methods and Applications*; Schrader, B., Ed.; Wiley-VCH: Weinheim, 1995; p 598.
(23) Hauser, M.; Oelichmann, J. *Mikrochim. Acta* **1988**, *1*, 39.
(24) Savitzky, A.; Golay, M. J. E. *Anal. Chem.* **1964**, *36*, 1627.
(25) Otto, M. *Chemometrics*; Wiley-VCH: Weinheim, 1999.
(26) Otto, A.; Korte, E. H. *Mikrochim. Acta* **1988**, *2*, 141.
(27) Nakamoto, K. *Infrared and Raman Spectra of Inorganic and Coordination Compounds*; Wiley: New York, 1986.

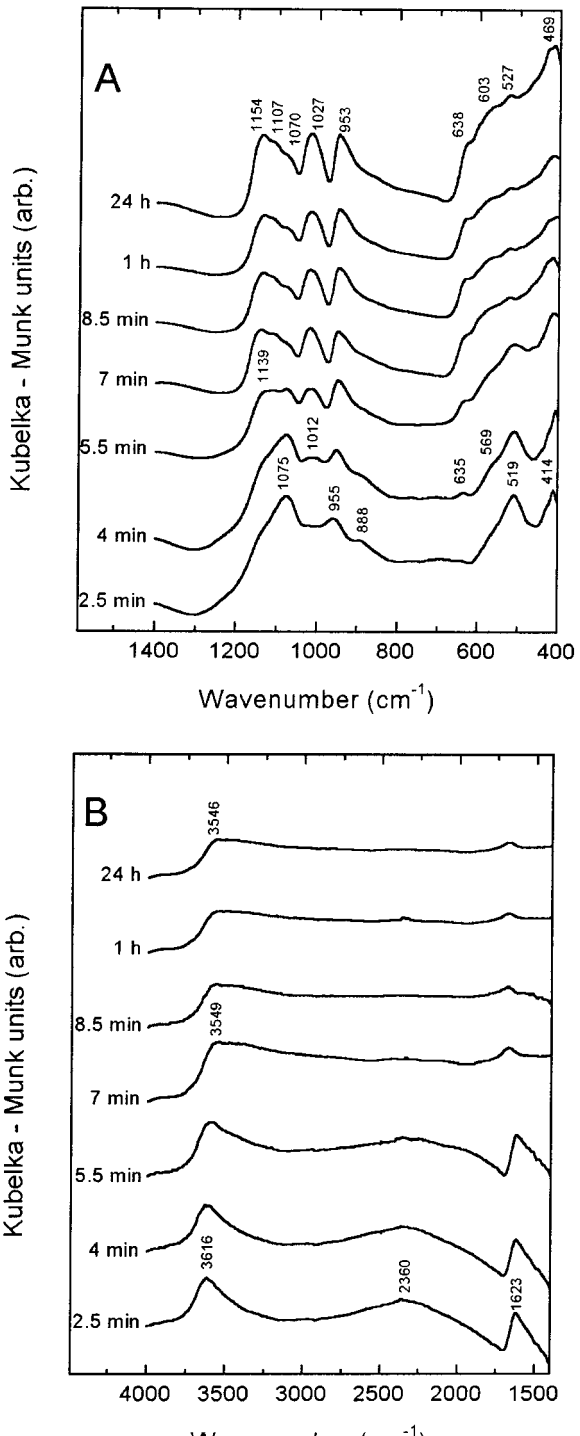

Figure 1. DRIFT spectra of unmodified ZPC: (A) spectra in the region 1400−400 cm^{-1} and (B) spectra in the region 4000−1400 cm^{-1}. Note that for reasons of clarity ordinate is scaled with ×3 magnification compared to spectra in part A.

indicate the precipitation of an amorphous phase since in the case of lack of translational symmetry the whole dispersion branch of the respective mode is allowed in the IR spectrum.[30] The observed bands at 1075, 955, 519, and 414 cm^{-1} are assigned to ν_{as}(P−O), ν_s(P−O),

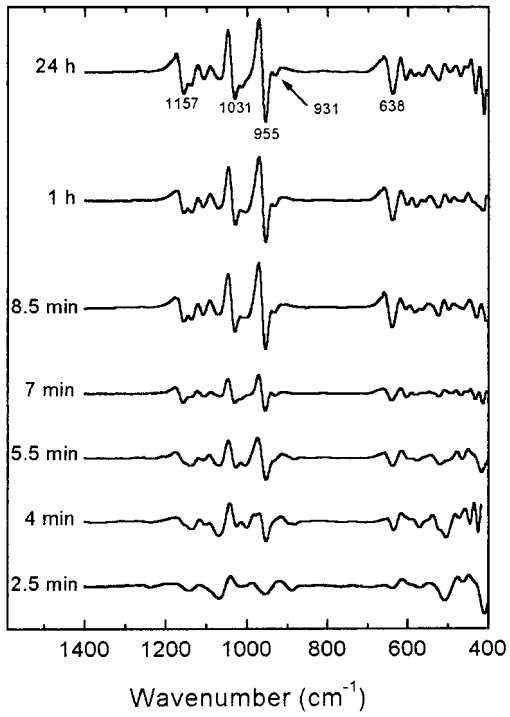

Figure 2. Second derivative spectra of unmodified ZPC in the range 1400−400 cm^{-1}.

δ_{as}(OPO), and δ_s(OPO), respectively. In the 4000−1400 cm^{-1} region water stretching modes ν(O−H) centered at 3616 cm^{-1}, and the water deformation mode δ(HOH) at 1623 cm^{-1}, as well as a broad vibrational absorption located at ∼ 2360 cm^{-1}, can be observed (Figure 1b). The latter band has been assigned to a combination mode ($2\nu_3+\nu_4$) of PO_4^{3-} fundamentals in the amorphous solid state.[31] Figure 1a displays that after 4 min from onset of mixing additional vibrational bands arise in the stretching and bending region of the phosphate ion. Their occurrence is ascribed to correlation field splitting, resulting from the formation of a crystalline phosphate and the concomitant lowering of the PO_4^{3-} site symmetry. This observation is distinctly more marked in the second derivative spectra. Progressive distortion of the PO_4^{3-} ion in the solid state leads to increased intensity and sharpness of these bands (Figure 2). This affects especially the ν_s(P−O) mode at 955 cm^{-1}, since this mode has very small or negligible splitting of transversal and longitudinal optic phonons of wavevector $q = 0$ in the crystalline solid state.[32] Hence, by several authors this mode of tetrahedral XO_4^{n-} ions has been used as a measure of the extent of distortion of the ions at the lower symmetric lattice site as compared to that of the free ion.[33,34] Upon proceeding reaction time, the maximum of the water stretching bands broadens and shows a significant shift to 3549 cm^{-1} after already 7 min (Figure 1b). Then, even up to 24 h, no further significant low-frequency shift can be observed. The main reason for these observations is the weakening of the intramolecular bonds of water, owing

(28) Farmer, V. C. *The Infrared Spectra of Minerals*; Adlard & Son Ltd.: Dorking, 1974.
(29) Martin, K. A.; Ferraro, J. R. *Appl. Spectrosc.* **1987**, *41*, 45.
(30) Henning, J.; Lutz, H. D.; Jacobs, H.; Mach, B. *J. Mol. Struct.* **1989**, *196*, 113.
(31) Dayanand, C.; Bhikshamaiah, G.; Jaya Tyagaraju, V.; Salagram, M.; Krishna Murty, A. S. R. *J. Mater. Sci.* **1996**, *31*, 1945.
(32) Decius, J. C.; Hexter, R. M. *Molecular Vibrations in Crystals*; McGraw-Hill: New York, 1977.
(33) Lutz, H. D.; Himmrich, J.; Schmidt, M. *J. Alloys Compd.* **1996**, *241*, 1.
(34) Petrusevski, V.; Soptrajanov, B. *J. Mol. Struct.* **1988**, *175*, 349.

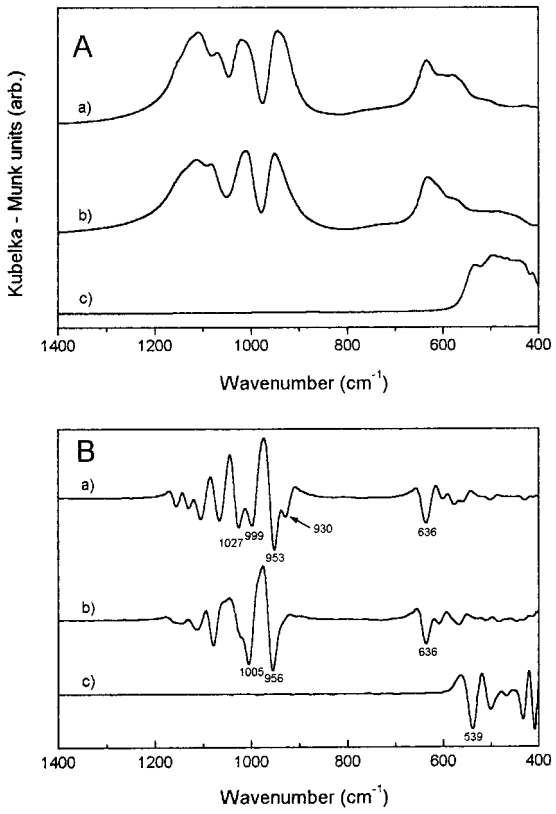

Figure 3. Reference spectra of polycrystalline (a) α-hopeite, (b) $Zn_3(PO_4)_2 \cdot 2H_2O$, and (c) ZnO: (A) DRIFT spectra in the region 1400−400 cm^{-1} and (B) second derivative spectra in the range 1400−400 cm^{-1}.

to the formation of hydrogen bonds. This results in a redshift of the bands since the respective internal force constants of water decrease and the anharmonicity of the vibrations increases.[35,36] Moreover, the PO_4^{3-} group in solid hydrates has a strong proton acceptor capability.[37] As established in the literature,[38] the energy of the H_2O bending mode increases with increasing strength of the hydrogen bonds (Figure 1b). The DRIFT and second derivative spectra of α-hopeite, $Zn_3(PO_4)_2 \cdot 2H_2O$, and ZnO are shown in Figure 3, parts a and b. In the second derivative spectrum of α-hopeite an important observation can be made in the 1200−900 cm^{-1} region, where the spectrum contains eight bands. Among these a weak, but pronounced, ν_s(P−O) mode of the PO_4^{3-} ion, found at 930 cm^{-1}, is an unambiguous indicator for α-hopeite. This component occurs due to correlation field splitting, rather than due to a sidelobe, generated by the Savitzky−Golay filter algorithm. In contrast to α-hopeite, the second derivative spectrum of $Zn_3(PO_4)_2 \cdot 2H_2O$ displays only a single ν_s(P−O) mode. Furthermore, α-hopeite exhibits a splitting into six ν_{as}(P−O) modes, compared to a splitting into almost five ν_{as}(P−O) modes for $Zn_3(PO_4)_2 \cdot 2H_2O$. The root cause of these distinctive features is the structural difference of the zinc phosphate hydrates. The orthophosphate α-hopeite crystallizes in the orthorhombic space group *Pnma* with $Z = 4$.[39] Important structural features are the division of zinc atoms in the ratio of 2:1 between ZnO_4 tetrahedra and $ZnO_2(H_2O)_4$ octahedra, sheets of which spread perpendicular to the [010] direction, separated by sheets of corner-sharing PO_4 and ZnO_4 tetrahedra. The PO_4 tetrahedra are all of equivalent symmetry C_1. Factor group analysis,[40] calculated for the stretching vibrations of the PO_4^{3-} ion in the α-hopeite structure, yields a splitting into three IR-active ν_s(P−O) modes, and nine IR-active ν_{as}(P−O) modes, respectively. However, only 8 of these 12 bands can be observed in Figure 2 since ZPC was investigated in the polycrystalline state. The crystal structure of $Zn_3(PO_4)_2 \cdot 2H_2O$ is not yet determined in detail although a Weissenberg study on a single crystal has already revealed the metric of the unit-cell.[41] When the reference spectra (Figure 3, parts a and b) are compared with the spectra of ZPC (Figures 1a and 2), α-hopeite as well as $Zn_3(PO_4)_2 \cdot 2H_2O$, which occurs as intermediate crystalline phase, can be clearly identified. In accordance with the literature,[42] polycrystalline zinc oxide shows a broad band centered at 460−450 cm^{-1} in the IR spectrum (Figure 3a). However, in the DRIFT spectra of ZPC (Figure 1a), the infrared bands of zinc oxide are obscured by the phosphate vibrations.

DRIFT Spectra for the Reaction between Zinc Oxide and Modified OPA. The DRIFT spectrum after 2.5 min shows the precipitation of an amorphous phosphate (Figure 4a). Vibrational bands located at 1079, 970, 517, and 419 cm^{-1} are attributed to the ν_{as}(P−O), ν_s(P−O), δ_{as}(POP), and δ_s(POP) modes of the PO_4^{3-} ion, respectively. In comparison to Figure 1a, the wavenumbers show a slight shift toward higher frequencies which is likely caused by the DRIFT sampling technique. In addition, a feature is found at 893 cm^{-1} (Figure 4a), and the derivative spectrum after 2.5 min exhibits weak but significant bands located at 767 and 677 cm^{-1} (Figure 5). Extensive infrared investigations on phosphorus compounds[43,44] indicate that P−O−P linkages of Q^2 type PO_4^{3-} tetrahedra exhibit characteristic IR bands near 900 and 700 cm^{-1}. Among the condensed phosphates cyclophosphates generally show characteristic absorptions near 900, 770, and 700 cm^{-1} which have been assigned to ν_{as}(POP), ν_s(POP), and harmonics of δ(POP), respectively.[31,43−46] Numerous IR studies on phosphate glasses, partly combined with ^{31}P MAS NMR and XPS investigations, have confirmed these assignments.[47−49] This strongly suggests the formation of an amorphous cyclophosphate which constitutes the matrix phase of modified ZPC. In fact, in the ternary system $ZnO-P_2O_5-H_2O$, $Zn_2P_4O_{12} \cdot 8H_2O$

(35) Lutz, H. D. *Struct. Bonding* **1988**, *69*, 97.
(36) Berglund, B.; Lindgren, J.; Tegenfeldt, J. *J. Mol. Struct.* **1978**, *43*, 169.
(37) Lutz, H. D.; Beckenkamp, K.; Möller, H. *J. Mol. Struct.* **1994**, *322*, 263.
(38) Falk, M. *Spectrochim. Acta A* **1984**, *40*, 43.
(39) Hill, R. J.; Jones, J. B. *Am. Mineral.* **1976**, *61*, 987.
(40) Fateley, W. G.; Dolish, F. R.; McDevitt, N. T.; Bentley, F. F. *Infrared and Raman Selection Rules for Molecular and Lattice Vibrations − The Correlation Method*; Wiley: New York, 1972.
(41) Arnaud, Y.; Sahakian, E.; Romand, M. *Appl. Surf. Sci.* **1988**, *32*, 281.
(42) McDevitt, N. T.; Baun, W. L. *Spectrochim. Acta* **1964**, *20*, 799.
(43) Bergmann, E. D.; Littauer, U. Z.; Pinchas, S. *J. Chem. Soc.* **1952**, *1*, 847.
(44) Corbridge, D. E. C.; Lowe, E. J. *J. Chem. Soc.* **1954**, *1*, 493.
(45) Steger, E. *Z. Anorg. Allg. Chem.* **1958**, *294*, 146.
(46) Meyer, K.; Hobert, H.; Barz, A.; Stachel, D. *Vibr. Spectrosc.* **1994**, *6*, 323.
(47) Brückner, R.; Chun, H. U.; Goretzki, H.; Sammet, M. *J. Non-Cryst. Solids* **1980**, *42*, 49.
(48) Hudgens, J. J.; Martin, S. W. *J. Am. Ceram. Soc.* **1993**, *76*, 1691.
(49) Khawaja, E. E.; Durrani, S. M. A.; Al-Adel, F. F.; Salim, M. A.; Sakhawat Hussain, M. *J. Mater. Sci.* **1995**, *30*, 225.

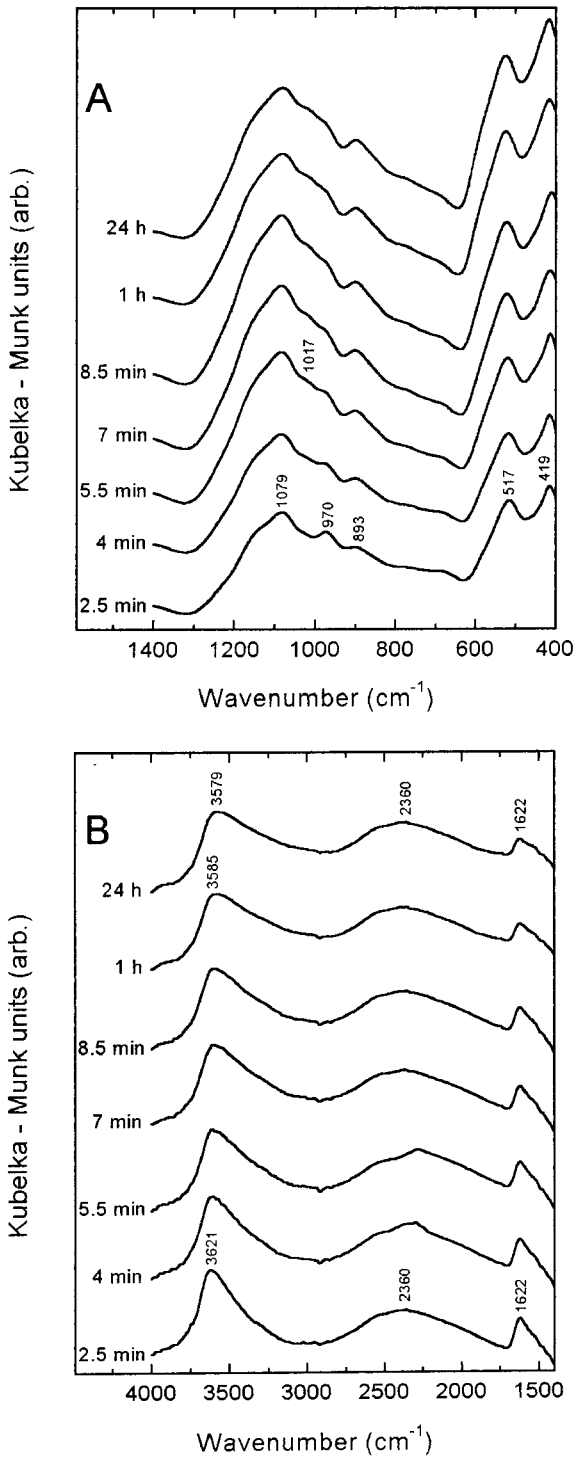

Figure 4. DRIFT spectra of modified ZPC: (A) Spectra in the region 1400−400 cm^{-1} and (B) spectra in the region 4000−1400 cm^{-1}. Note that for reasons of clarity ordinate is scaled with ×3 magnification compared to spectra in part A.

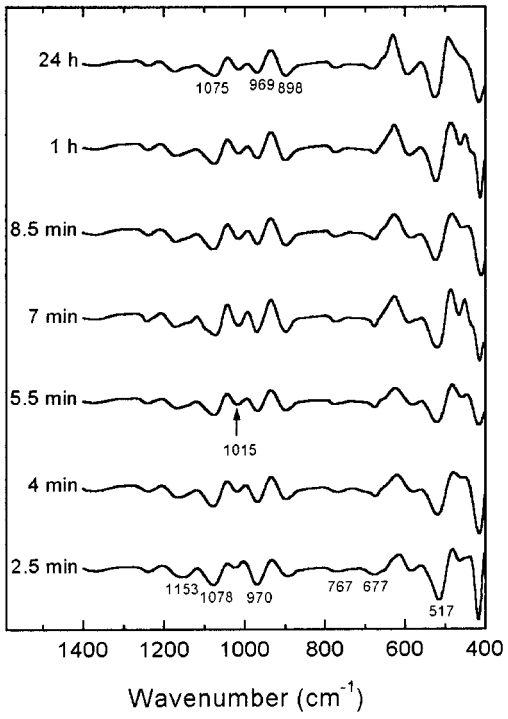

Figure 5. Second derivative spectra of modified ZPC in the range 1400−400 cm^{-1}.

crystallizes as a cyclotetraphosphate under ambient conditions.[50] In the structure, zinc atoms are octahedrally coordinated and divide in the ratio 1:1 between $ZnO_4(H_2O)_2$ and $ZnO_2(H_2O)_4$ octahedra which spread in the (001) plane. These layers are linked by $P_4O_{12}^{4-}$ cyclotetraphosphate anions. The PO_4 tetrahedra are all of equivalent site symmetry C_1. Thus, in accordance with the Sato−Grutzeck model for strength in cement forming systems,[51] the high strength of modified ZPC, in contrast to the well-known brittleness of unmodified ZPC, is brought about by the formation of a condensed anion structure.

Upon proceeding reaction time, the bands retain constant intensity and frequency, even after 24 h (Figure 4a). However, after 5.5 min, a band arises at 1017 cm^{-1}. This observation points to a crystallization of the metastable cyclophosphate phase, running with a noticeable sluggish kinetic. In the 4000−1400 cm^{-1} region, bands at 3621, 2360, and 1622 cm^{-1} can be clearly recognized (Figure 4b). They are assigned to water stretching bands ν(O−H), PO_4^{3-} combination mode ($2\nu_3+\nu_4$), and the water bending mode δ(HOH). The hydration of the amorphous matrix phase leads to a redshift of the water stretching band maximum to 3585 cm^{-1} after 1 h. Even when stored at physiological temperature and 100% relative humidity, the hydration is by far slowed after 1 h since the maximum of the water stretching bands is located at 3579 cm^{-1} after 24 h. The second derivative spectra do not show further important details (Figure 5). It is generally accepted that hydrated cyclophosphates are exceptional among inorganic phosphate hydrates in that the maxima of the water stretching bands can be found at wavenumbers as high as 3580 cm^{-1} in some salts.[44] It is apparent, therefore, that in these compounds, some, at least, of the water molecules are only loosely held in the crystal lattice. This actually holds for $Zn_2P_4O_{12}\cdot 8H_2O$ where the structure refinement yielded a large isotropic temperature factor for one of the water molecules.[50] It has been concluded that this water molecule is scarcely involved in hydrogen bonding.

Considering these results, the band observed at 885 cm^{-1} in the DRIFT spectrum of unmodified ZPC (Figure

(50) Averbuch-Pouchot, M. T. *Z. Anorg. Allg. Chem.* **1983**, *503*, 231.

(51) Sato, H.; Grutzeck, M. *Proc. Mater. Res. Soc.* **1992**, *245*, 235.

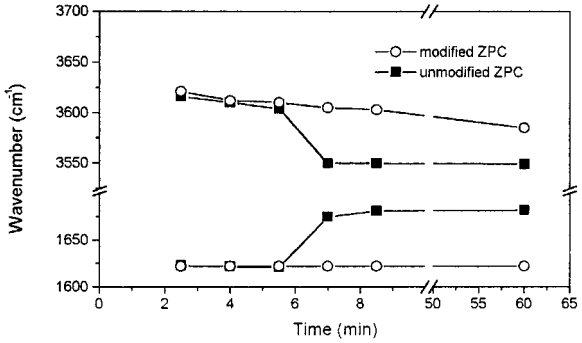

Figure 6. Evolution of maximum of water stretching and deformation bands for unmodified and modified ZPC.

1a) may also be attributed to the ν_{as}(POP) mode of amorphous $Zn_2P_4O_{12}\cdot 8H_2O$. This band is no longer detectable after 7 min since crystallization of $Zn_3(PO_4)_2\cdot 2H_2O$ takes place rapidly. However, as a certain fraction of $Zn_2P_4O_{12}\cdot 8H_2O$ has already transformed after 2.5 min the remaining characteristic infrared bands of this compound are not distinctly detectable in Figures 1a and 2.

The metastable state of the matrix of modified ZPC can be visualized by plotting the maximum of the water stretching and deformation bands versus reaction time (Figure 6). An important result is that the initial formation of the cyclotetraphosphate phase seems to proceed with similar rate constants for unmodified and modified ZPC. The maximum of the water stretching bands shows a drastic decrease upon crystallization of unmodified ZPC. For modified ZPC these bands retain high frequency, indicating that hydration is slowed and crystallization proceeds with sluggish kinetics. The reverse holds for the water deformation bands. Thus, water in unmodified ZPC is more strongly bound to the matrix phase. This conclusion can also be drawn from the thermoanalytical investigations. On heating, modified ZPC loses all its water of hydration already at an onset temperature of 343 K, whereas unmodified ZPC shows an α-hopeite like dehydration behavior, and water is lost in three stages at 416, 457, and 503 K, respectively (Figure 7a). The thermogravimetric curves show conspicuous similarity (Figure 7b).

In contrast to the DRIFT technique, Raman spectroscopy reveals the composite nature of ZPC, since the characteristic vibrations of residual zinc oxide, embedded in an amorphous or crystalline phosphate matrix, can be clearly seen (Figure 8). The Raman spectrum of modified ZPC shows a band at 437 cm^{-1} which is assigned to the E_2 mode of the hexagonal wurtzite phase of zinc oxide.[52] Broad bands centered at 924, 1009, and 1108 cm^{-1} are due to amorphous $Zn_2P_4O_{12}\cdot 8H_2O$. In addition to the E_2 mode of zinc oxide the Raman spectrum of unmodified ZPC exhibits the characteristic bands of crystalline α-hopeite, located at 941, 996, 1056, and 1147 cm^{-1}. The band at 996 cm^{-1} is assigned to the ν_s(P−O) mode, and the remaining bands are ν_{as}(P−O) modes of the PO_4^{3-} ion. A comparison of infrared and Raman frequencies of crystalline ZPC shows that there is lack of coincidence. This is attributed to mutual exclusion between the infrared and Raman frequencies, due to the centric space group of α-hopeite.

(52) Exarhos, G. J.; Sharma, S. K. *Thin Solid Films* **1995**, *270*, 27.

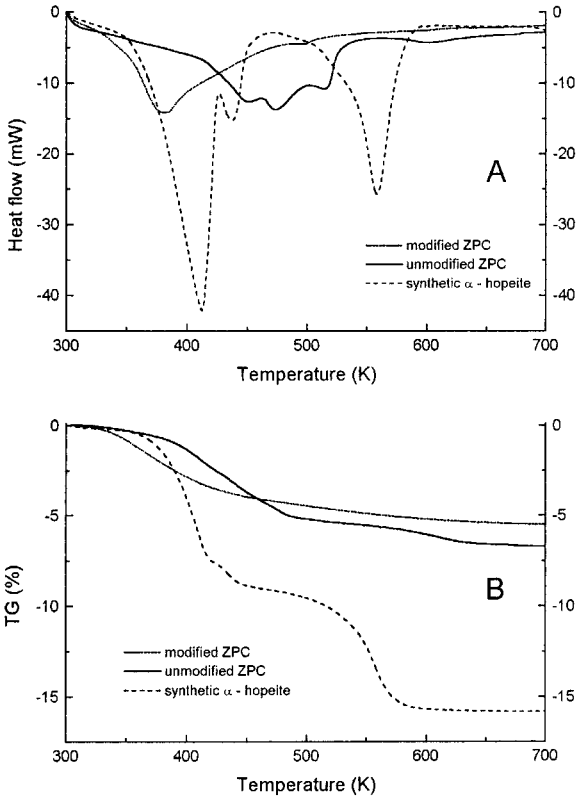

Figure 7. Thermoanalytical investigation of 24 h matured ZPC: (A) DTA curves and (B) TG curves.

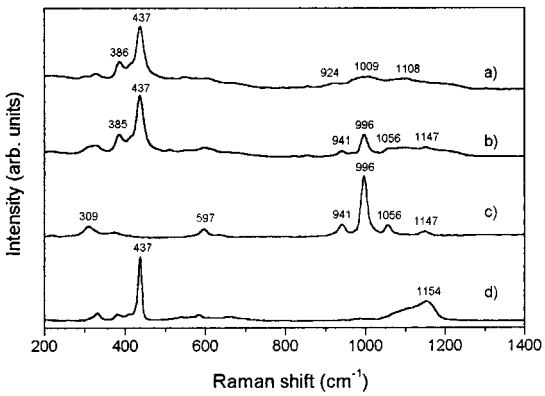

Figure 8. Raman spectra of (a) modified ZPC, (b) unmodified ZPC, (c) α-hopeite, and (d) zinc oxide.

Phase Sequence and Reaction Mechanism for ZPC Prepared from Unmodified OPA. To clarify aspects of the chemical evolution of ZPC, knowledge of chemical equilibria in the ternary system $ZnO-P_2O_5-H_2O$ is required. Therefore, the phase diagram at ambient conditions (Figure 9) was calculated from data given in the literature.[53−55] No attempt has been made to fully demarcate and label the phase fields because there are no data available concerning the interrelationships of the several hydrates. When the cement powder and the liquid are mixed, zinc cations are released upon protonation of oxygen surface sites of zinc oxide. In diluted acids the divalent zinc ion becomes surrounded

(53) Eberly, N. E.; Gross, C. V.; Crowell, W. S. *J. Am. Chem. Soc.* **1920**, *42*, 1433.
(54) Salmon, J. E.; Terrey, H. *J. Chem. Soc.* **1950**, *3*, 2813.
(55) Goloshchapov, M. V.; Filatova, T. N. *Russ. J. Inorg. Chem.* **1969**, *14*, 424.

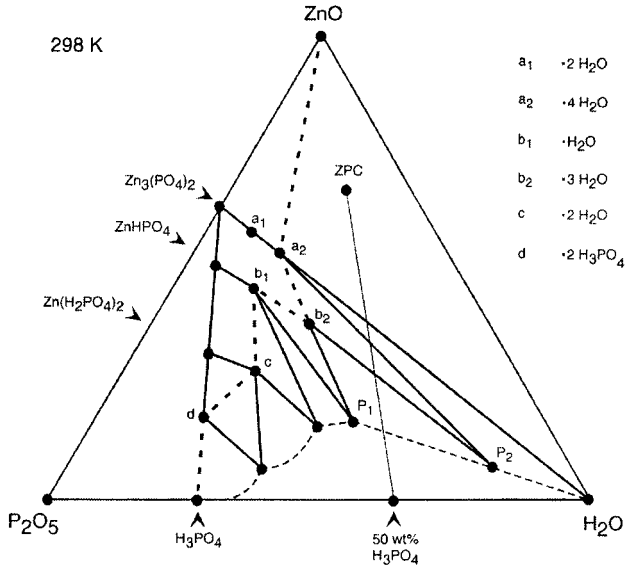

Figure 9. The ternary system ZnO−P_2O_5−H_2O at 298 K and 101.3 kPa. Thick dashed line represents solidus; thin dashed line represents liquidus. Point ZPC represents final composition of unmodified ZPC when a powder-to-liquid ratio of 2.0 is used.

by an inner hydration sheath and solubilizes by forming aquo complexes, $Zn(H_2O)_n^{2+}$ with *n* equal four or six.[56] However, the acid component of ZPC is of sufficient concentration to expect predominantly the formation of simple zinc phosphate salts, which has already been confirmed by a ^{31}P NMR study on 50 wt % OPA.[57] To give an indication of the early cement forming reactions prior to gelation, it is essential to take the chemical speciation in 50 wt % (∼10.2 m) OPA into consideration. Although some models for OPA have been reported,[58−60] they fitted the experimentally determined activities of water only for molalities far below 10 mol kg^{-1}. However, a recently presented model[61] fits the activities of water up to an overall molality of 24 mol kg^{-1}. This model includes the species H_3PO_4, $H_2PO_4^-$, and the $H_5P_2O_8^-$ ion, earlier proposed to be present in more concentrated OPA.[58,62] According to this model the concentration ratio of the anions $H_5P_2O_8^-$ and $H_2PO_4^-$ is ∼9:1 in 50 wt % OPA. Thus, the early stages of reaction may be governed by the dissociation of the ionic species $H_5P_2O_8^-$ and the reaction between zinc cations and $H_2PO_4^-$ counterions in solution near the solid liquid interface:

$$Zn^{2+}(aq) + 2H_5P_2O_8^-(aq) \rightarrow Zn(H_2PO_4)_2(aq) + 2H_3PO_4(l) \quad (1)$$

$$Zn^{2+}(aq) + 2H_2PO_4^-(aq) \rightarrow Zn(H_2PO_4)_2(aq) \quad (2)$$

Assuming thermodynamic equilibrium, the continued incorporation of zinc in OPA represents an approach to the liquidus and can only result in the precipitation of $ZnHPO_4{\cdot}3H_2O$ (Figure 9). As more zinc oxide is incorporated in the mix, so more $ZnHPO_4{\cdot}3H_2O$ is precipitated, while the nominal acid concentration declines, following the liquidus from the isothermal invariant point P1 toward P2, when α-hopeite becomes the precipitated phase:

$$3ZnHPO_4{\cdot}3H_2O(s) \rightarrow Zn_3(PO_4)_2{\cdot}4H_2O(s) + H_3PO_4(l) + 5H_2O(l) \quad (3)$$

However, the DRIFT spectra unambiguously show that setting of ZPC is a sequence of transformations far from thermodynamic equilibrium. It is plausible that dizinc cyclotetraphosphate octahydrate ($Zn_2P_4O_{12}{\cdot}8H_2O$ = 2 $Zn(H_2PO_4)_2{\cdot}2H_2O$) starts to precipitate out, once a critical concentration above the solubility limit has been reached:

$$Zn(H_2PO_4)_2(aq) + 2H_2O(l) \rightarrow Zn(H_2PO_4)_2{\cdot}2H_2O(s) \quad (4)$$

Although not directly evident from our DRIFT spectra the solid-state transformation to intermediate zinc hydrophosphate monohydrate, which has been shown to form on dehydration of $Zn_2P_4O_{12}{\cdot}8H_2O$,[63] has to be taken into account. This would also be in agreement with the phase relationships in the respective part of the ternary system. Thus, further transformations indicate an increasing Zn/P ratio of the matrix phase from 0.5 to 1.5, when the formation of α-hopeite completes the phase sequence:

$$Zn(H_2PO_4)_2{\cdot}2H_2O(s) \rightarrow ZnHPO_4{\cdot}H_2O(s) + H_3PO_4(l) + H_2O(l) \quad (5)$$

$$3ZnHPO_4{\cdot}H_2O(s) \rightarrow Zn_3(PO_4)_2{\cdot}2H_2O(s) + H_3PO_4(l) + H_2O(l) \quad (6)$$

$$Zn_3(PO_4)_2{\cdot}2H_2O(s) + 2H_2O(l) \rightarrow Zn_3(PO_4)_2{\cdot}4H_2O(s) \quad (7)$$

Inspection of this scheme clearly indicates that the overall reaction:

$$3ZnO(s) + 2H_3PO_4(l) + H_2O(l) \rightarrow Zn_3(PO_4)_2{\cdot}4H_2O(s) \quad (8)$$

can be separated into initial Lewis acid−base reactions (eqs 1 and 2), and subsequent stages of hydration (eqs 4−7). It has been reported that the $Zn_3(PO_4)_2{\cdot}2H_2O$ framework is 29.7 kJ/mol less stable in enthalpy of formation than α-hopeite,[64,65] which might also account for the above phase sequence. However, the initial formation of amorphous $Zn_2P_4O_{12}{\cdot}8H_2O$ is surprising since the P−O−P linkage of condensed phosphates is known to be hydrolytically instable.[66] Macroscopic thermodynamic dictates that the phase that is formed

(56) Ziemniak, S. E.; Jones, M. E.; Combs, K. E. S. *J. Solution Chem.* **1992**, *21*, 1153.
(57) O'Neill, I. K.; Prosser, H. J.; Richards, C. P.; Wilson, A. D. *J. Biomed. Mater. Res.* **1982**, *16*, 39.
(58) Elmore, K. L.; Hatfield, J. D.; Dunn, R. L.; Jones, A. D. *J. Phys. Chem.* **1965**, *69*, 3520.
(59) Pitzer, K. S.; Silvester, L. F. *J. Solution Chem.* **1976**, *5*, 269.
(60) Rumpf, B.; Maurer, G. *J. Solution Chem.* **1994**, *23*, 37.
(61) Jiang, C. *Chem. Eng. Sci.* **1996**, *5*, 689.
(62) Childs, C. W. *J. Phys. Chem.* **1969**, *75*, 2956.
(63) Samuskevich, V. V.; Lukyanchenko, O. A.; Samuskevich, L. N. *Ind. Eng. Chem. Res.* **1997**, *36*, 4791.
(64) Al-Maydama, H. M. A.; Gardner, P. J.; McAra, I. W. *Thermochim. Acta* **1992**, *194*, 117.
(65) Al-Maydama, H. M. A.; Gardner, P. J.; McAra, I. W. *Thermochim. Acta* **1992**, *196*, 117.
(66) Corbridge, D. E. C. Phosphorous, an Outline of its Chemistry, Biochemistry and Technology. In *Studies in Inorganic Chemistry*; Elsevier: Amsterdam, 1990; Vol 10.

in a supersaturated system is the one that has the lowest free energy. However, homogeneous nucleation is an essentially dynamic process, and therefore one cannot expect a priori that on supersaturation the system, the thermodynamically most stable phase, here α-hopeite, will formed.[67,68] If the α-hopeite phase has a different structure to the supersaturated solution the interface will be incoherent with a high interfacial energy. Therefore, the activation energy for nucleation will be high and homogeneous nucleaction of the stable α-hopeite phase highly improbable. In classical nucleation theory, the resulting free energy is determined by the surface free energy, the density of the precipitate, and the difference in chemical potential between the precipitate and the supersaturated solution. Observations of such systems show that a metastable route does often exist and the overall sequence of phases which nucleate under nonequilibrium conditions is one of a stepwise approach toward the equilibrium structure and composition, rather than a single-step nucleation of the stable phase which involves a large activation energy barrier.[69] When the transition phases have a structure similar to the supersaturated solution a coherent or semicoherent interface can be formed, thereby reducing the activation energy for nucleation. This concept has been known as the Ostwald step rule for many years.[70] Since the structural flexibility of the $P_4O_{12}^{4-}$ ion is well documented,[45] a properly adjusted conformation of this ion may thus play the key role in the coagulation of the $Zn_2P_4O_{12}\cdot 8H_2O$ matrix phase.

Phase Sequence and Reaction Mechanism for ZPC Prepared from Modified OPA. For clinical practice, the incorporation of aluminum into the cement liquid is of importance for enhancement of compressive strength,[71] for reduction of heat generation, and for setting prolongation to ensure sufficient working time in the surgery.[72] The addition of zinc to the cement liquid leads to further setting prolongation and biocompatible heat generation during setting.[72] Moreover, for the first time we have observed in this study that surface roughness of ZPC is effectively reduced upon modification of the cement liquid. This allows closer adaption of the material to human dentine and enamel. Here, a typical sample of modified ZPC exhibits a surface roughness of 566 nm in contrast to 892 nm, in the case of unmodified ZPC (Figure 10). Crystal faces of α-hopeite can be clearly seen on the surface of unmodified ZPC film.

The addition of aluminum profoundly affects the setting chemistry of ZPC. While there is absence of any complexing of zinc by OPA, the formation of complexes between aluminum and phosphate species has long been known.[73,74] Molecular dynamic simulations combined with ^{27}Al and ^{31}P NMR investigations[75] on aluminum-

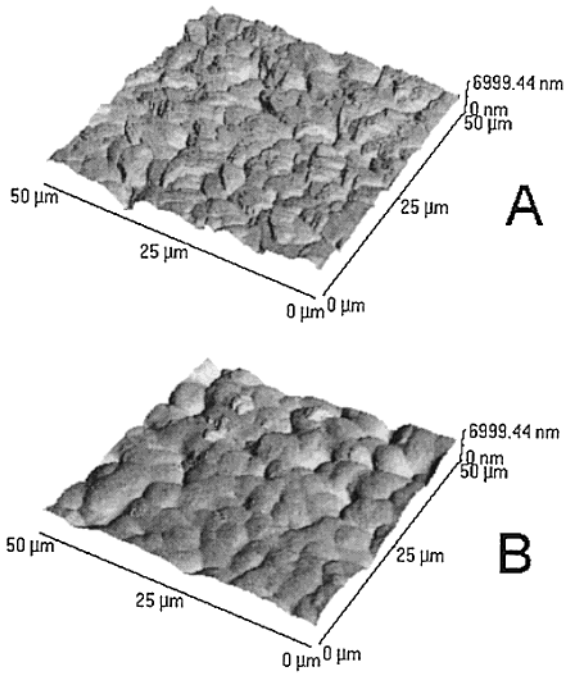

Figure 10. AFM images of 24 h matured ZPC films: (A) unmodified ZPC, (B) modified ZPC.

containing OPA, with P/Al ranges between 0.1 and 20, showed the presence of the complexes $[Al(H_2O)_5(H_3PO_4)]^{3+}$, $[Al(H_2O)_5(H_3PO_4)_n]^{m+}$ ($n \geq 2$, m is undetermined), $[Al(H_2O)_5(H_2PO_4)]^{2+}$, and $[Al(H_2O)_4(H_2PO_4)_2]^{+}$ for pH below 1.5. However, amorphous aluminophosphate hydrogels were formed for pH $\approx 2-10$ and the range of pHs over which stable gels existed turned out to increase with increasing P/Al ratios.[76] Since the typical pH of a fresh ZPC paste, mixed from modified OPA using a powder-to-liquid ratio of 2.0, is in the range of 3 to 3.5 after 2 min from onset of mixing,[71] the presence of aluminophosphate complexes as well as their aggregation to a hydrogel have to be taken into account. This implies the formation of an aluminophosphate hydrogel, embedding zinc phosphate hydrate coated zinc oxide particles upon neutralization, rather than the formation of a hypothetical solid solution $Zn_{3-3x}Al_{2x}(PO_4)_2\cdot 4H_2O$ because ^{31}P NMR studies on in vivo matured ZPC showed only evidence of an uptake of magnesium cations in the α-hopeite lattice.[17] Hence, a phase separation between aluminophosphate hydrogel and zinc phosphate hydrates occurs during setting. In some respect the chemical evolution of modified ZPC shows striking similarities to the formation of aluminophosphate zeolitic materials. These molecular sieves are synthesized under acidic or neutral hydrothermal conditions and their amorphous aluminophosphate gel precursor phase can only be crystallized on a laboratory time scale when organic templates are added as structure directing agents.[77,78] Concerning the early stages of reaction a model has been proposed for the formation of aluminophosphates in which two- and three-dimen-

(67) Glansdorff, P.; Prigogine, I. *Thermodynamic Theory of Structure, Stability and Fluctuations*; Wiley: New York, 1971.
(68) Feenstra, T. P.; De Bruyn, P. L. *J. Coll. Interface Sci.* **1981**, *84* (1), 66.
(69) Saito, Y. *Statistical Physics of Crystal Growth*; World Scientific: Singapore, 1996.
(70) Ostwald, W. *Z. Phys. Chem.* **1897**, *22*, 289.
(71) Park, C. K.; Silsbee, M. R.; Roy, D. M. *Cem. Concr. Res.* **1998**, *28*, 141.
(72) Pawlig, O.; Trettin, R. *Thermochim. Acta* **1999**, *329*, 7.
(73) Jameson, R. F.; Salmon, J. E. *J. Chem. Soc.* **1954**, 4013.
(74) Akitt, J. W.; Greenwood, N. N.; Lester, G. D. *J. Chem. Soc. A* **1971**, 2450.
(75) Mortlock, R. F.; Bell, A. T.; Radke, C. J. *J. Phys. Chem.* **1993**, *97*, 767.
(76) Mortlock, R. F.; Bell, A. T.; Radke, C. J. *J. Phys. Chem.* **1993**, *97*, 775.
(77) Garcia Carmona, J.; Rodriguez Clemente, R.; Gomez Morales, J. *Adv. Mater.* **1998**, *10*, 468.
(78) Francis, R. J.; O'Hare, D. *J. Chem. Soc., Dalton. Trans.* **1998**, *19*, 3133.

sional structures are formed via hydrolysis and condensation of an initial parent chain structure which forms first,[79,80] even in aqueous systems at room temperature.[81] The presence of water evidently catalyzes the subsequent hydrolysis and transformation of the chain to branched structures on rendering the medium neutral or alkaline.[80] It would be reasonable here, that these chains entangle already precipitated $Zn_2P_4O_{12}\cdot 8H_2O$ building units of colloidal size, thereby preventing from their rapid growth and crystallization by providing steric hindrance. Certainly, under the high humidity in oral environment, hydrolysis of these chains can take place with simultaneous lifting of steric hindrance. Thus, further reconstruction of the metastable matrix and hydration of the final α-hopeite phase is completed with sluggish kinetics. In particular, our proposed reaction mechanism for the chemical evolution of modified, as well as of unmodified, ZPC postulates a topochemical solid hydrogel transformation.

Acknowledgment. This research was financially supported by the Stiftung Rheinland-Pfalz für Innovation. We thank Dr. L. Nasdala, who performed the Raman experiments, and Professor H. D. Lutz for helpful discussions.

CM991148O

(79) Oliver, S.; Kuperman, A.; Lough, A.; Ozin, G. A. *Chem. Mater.* **1996**, *8*, 2391.
(80) Oliver, S.; Kuperman, A.; Ozin, G. A. *Angew. Chem., Int. Ed.* **1998**, *37*, 46.
(81) Tieli, W.; Long, Y.; Wengin, P. *J. Solid State Chem.* **1990**, *89*, 392.